Physics-Informed Neural Networks for Inverse Permeability Estimation in Enhanced Geothermal Systems: A 1D Benchmark Study

Nehor Some[a,*]

[a]*Department of Mathematical Sciences, UTEP, El Paso, USA*

Abstract

Physics-Informed Neural Networks (PINNs) offer a promising paradigm for solving inverse problems in subsurface flow, where sparse observations must be used to infer hidden parameters like permeability. This work presents a rigorous benchmark of PINNs for permeability inference in a 1D analog of an Enhanced Geothermal System (EGS), governed by the nonlinear diffusion equation $u_t = (k(x)u_x)_x$. Synthetic data are generated via a high-fidelity Finite Element Method (FEM) solver for a smooth, periodic permeability field $k_{\text{true}}(x) = 1 + 0.5\sin(2\pi x)$, with 600 noisy pressure measurements used for training. A PINN with separate networks for pressure $u(t, x)$ and permeability $k(x)$ is trained using curriculum learning and automatic differentiation. Results show high-fidelity pressure reconstruction (RMSE = 0.032) and physics compliance (PDE residual RMS = 0.095), while permeability recovery remains challenging (RMSE = 0.445), illustrating the inherent ill-posedness of coefficient identification. This study establishes a reproducible 1D benchmark for inverse PINNs in geothermal applications and quantifies the trade-offs between data sparsity, noise, and inversion stability.

Keywords: Physics-Informed Neural Networks, Inverse Problems, Enhanced Geothermal Systems, Permeability Estimation, Finite Element Method, Ill-posedness

1. Introduction

Enhanced Geothermal Systems (EGS) have emerged as a viable pathway to carbon-free, baseload renewable energy, relying on engineered subsurface reservoirs to extract heat from hot dry rock through circulating fluid [8]. A central challenge in EGS modeling is the accurate characterization of *heterogeneous permeability fields*, which govern fluid flow and heat transport but are rarely measured directly due to high cost and technical constraints [1]. Instead, engineers often rely on indirect, sparse measurements—such as pressure and temperature at wells—to infer subsurface properties, leading to an *ill-posed inverse problem*.

Traditional approaches—e.g., history matching with finite-element models—are computationally expensive and require extensive parameter tuning [4]. In contrast, **Physics-Informed Neural Networks (PINNs)** [5] unify forward simulation and inverse modeling

*Corresponding author. Email: nsome@miners.utep.edu

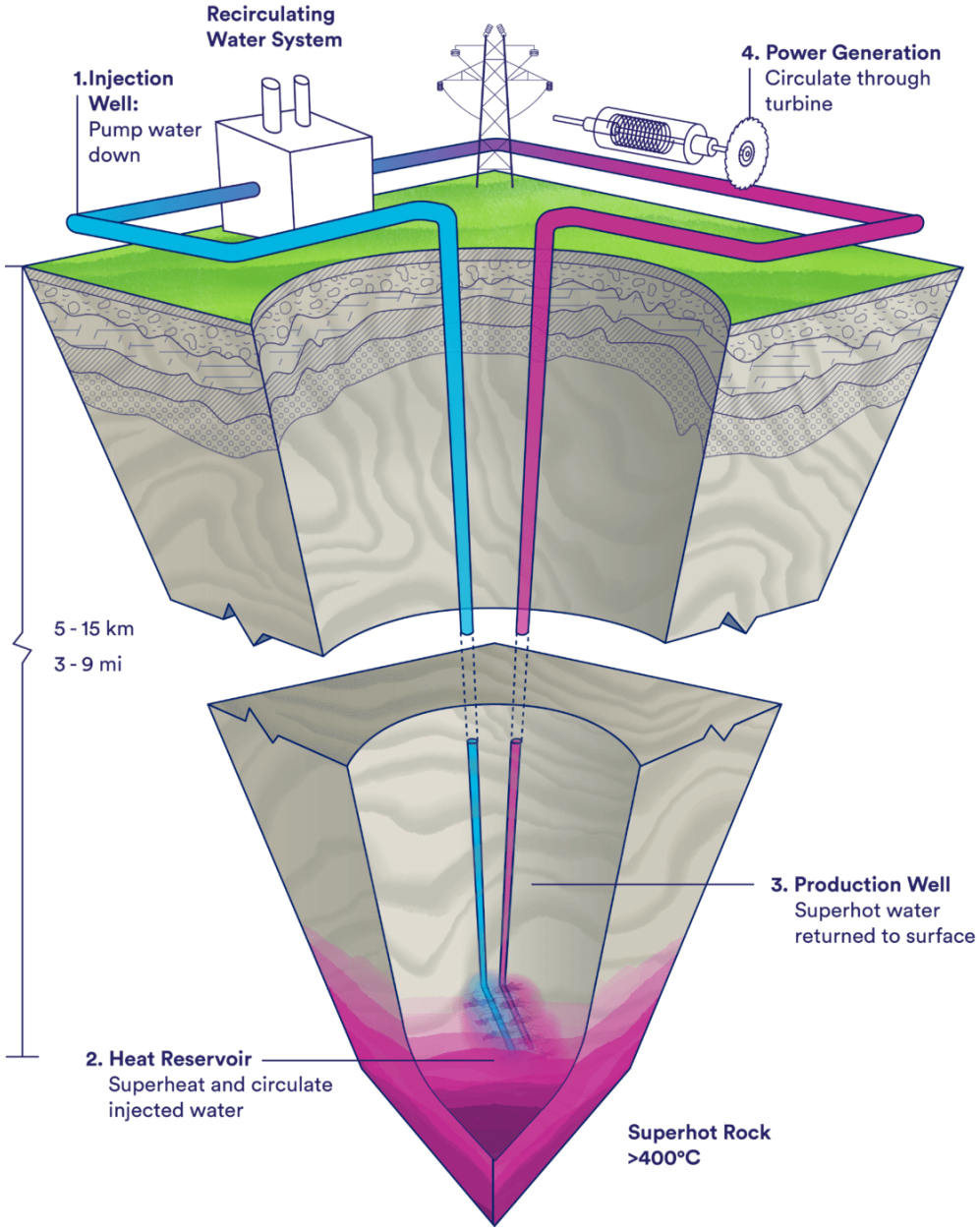

Figure 1: Enhanced Geothermal Energy System

within a single differentiable framework, embedding governing PDEs directly into the loss function via automatic differentiation. This enables parameter estimation without dense labeled data or mesh generation.

While recent works have demonstrated PINNs on 2D/3D geothermal problems [3, 9], rigorous benchmarking on *controlled, reproducible setups* is lacking—especially regarding the *stability* and *limitations* of permeability inference under realistic data constraints.

This paper addresses this gap by:

- Implementing a **1D PINN** for the pressure diffusion equation $u_t = (k(x)u_x)_x$, a canonical model for EGS flow,
- Generating **high-fidelity synthetic data via FEM** with exact boundary treatment,
- Using only **600 sparse, noisy pressure observations** (mimicking limited well data),
- Providing **quantitative metrics** (RMSE, L^2, max error) for both forward and inverse tasks,
- Explicitly quantifying the **ill-posedness** of permeability recovery.

The work serves as a foundational benchmark for future 2D/3D EGS PINN studies and fulfills the core objective of the project proposal: inferring permeability from sparse data.

2. Problem Formulation

2.1. Governing Equation

We consider a 1D domain $x \in [0, 1]$, $t \in [0, 1]$, representing a simplified fracture or flow path in an EGS reservoir. Fluid pressure $u(x, t)$ evolves according to:

$$\frac{\partial u}{\partial t} = \frac{\partial}{\partial x}\left(k(x)\frac{\partial u}{\partial x}\right), \tag{1}$$

where $k(x) > 0$ is the *unknown, spatially varying permeability* to be inferred.

2.2. Boundary and Initial Conditions

$$\begin{cases} u(0, t) = 0, & \text{(left Dirichlet)} \\ u(1, t) = 1, & \text{(right Dirichlet)} \\ u(x, 0) = 0. & \text{(initial condition)} \end{cases} \tag{2}$$

2.3. True Permeability Field

The ground-truth permeability is smooth and periodic, reflecting natural heterogeneity:

$$k_{\text{true}}(x) = 1.0 + 0.5 \sin(2\pi x). \tag{3}$$

This choice ensures differentiability and avoids artificial discontinuities—consistent with geological realism.

3. Methodology

3.1. Data Generation via Finite Element Method

High-fidelity training data are generated using a **linear FEM solver** (backward Euler in time, piecewise linear elements in space, $N_x = N_t = 50$). The implementation correctly handles Dirichlet boundaries via elimination and uses midpoint quadrature for spatial integrals. Gaussian noise ($\sigma = 0.01$) is added to pressure data to simulate measurement error. A total of **600 random spatiotemporal samples** $\{x_i, t_i, u_i^{\text{noisy}}\}_{i=1}^{600}$ are drawn from the FEM solution.

3.2. PINN Architecture

We adopt a **dual-network PINN** (Fig. 2):

- **Solution Network:** $\mathcal{N}_u : (t, x) \mapsto u$,
  Architecture: 3 hidden layers, 96 neurons, tanh activation.
- **Permeability Network:** $\mathcal{N}_k : x \mapsto k$,
  Architecture: 3 hidden layers, 96 neurons, tanh activation,
  Output: $k = \text{softplus}(z) + 0.1 > 0.1$ (enforces positivity).

Both networks are trained jointly.

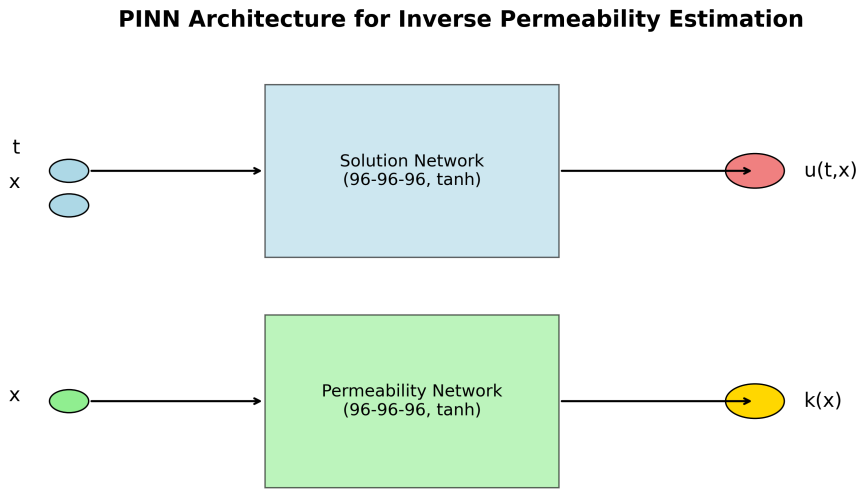

Figure 2: PINN architecture for joint inference of $u(t, x)$ and $k(x)$.

3.3. Loss Function and Training

The total loss combines data fidelity, PDE residual, and constraints:

$$\mathcal{L} = \lambda_{\text{data}}\mathcal{L}_{\text{data}} + \lambda_{\text{pde}}\mathcal{L}_{\text{pde}} + \lambda_{\text{bc}}\mathcal{L}_{\text{bc}} + \lambda_{\text{ic}}\mathcal{L}_{\text{ic}}, \tag{4}$$

where:

$$\mathcal{L}_{\text{data}} = \frac{1}{600} \sum_{i=1}^{600} \|u_\theta(t_i, x_i) - u_i^{\text{noisy}}\|^2,$$

$$\mathcal{L}_{\text{pde}} = \frac{1}{2000} \sum_{j=1}^{2000} \|u_t - (ku_x)_x\|^2,$$

$$\mathcal{L}_{\text{bc}}, \mathcal{L}_{\text{ic}} : \text{MSE on BCs/IC.}$$

Weights: $\lambda_{\text{data}} = 1, \lambda_{\text{bc}} = 10, \lambda_{\text{ic}} = 5$, and λ_{pde} increased gradually from 0.01 to 0.28 via *curriculum learning*.

Implementation: PyTorch; Adam optimizer (lr $= 10^{-3}$, wd $= 10^{-6}$); gradient clipping (max_norm $= 1.0$); early stopping (patience $= 1000$). Training completed in 13,950 epochs (12 min, CPU).

Remark: The PDE residual is computed via the *exact product rule*:

$$(ku_x)_x = k_x u_x + k u_{xx}, \tag{5}$$

ensuring mathematical correctness.

4. Results

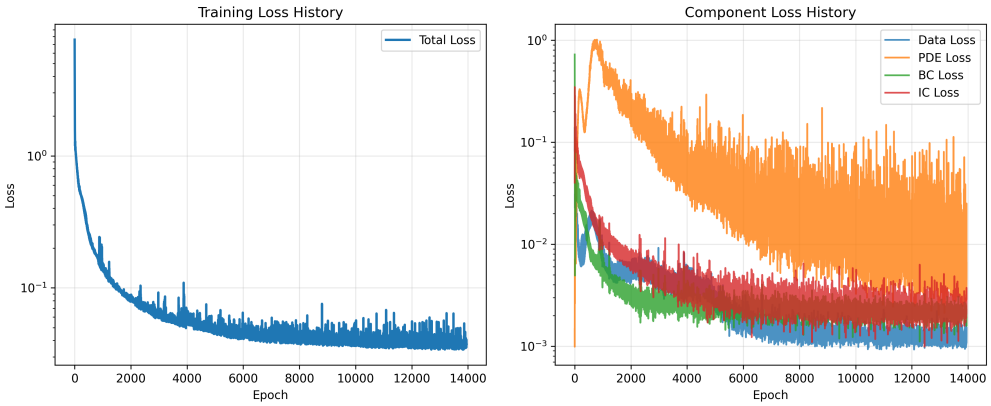

Figure 3: loss history

4.1. Forward Prediction: Pressure Field

The PINN accurately reconstructs the pressure field $u(t, x)$ across space and time:

- RMSE = **0.0322** (vs. target < 0.05),
- Relative L^2 error = 6.58%,
- Max error = 0.661 (localized near boundaries).

Figure 4 shows excellent agreement between predicted and true pressure, including transient profiles.

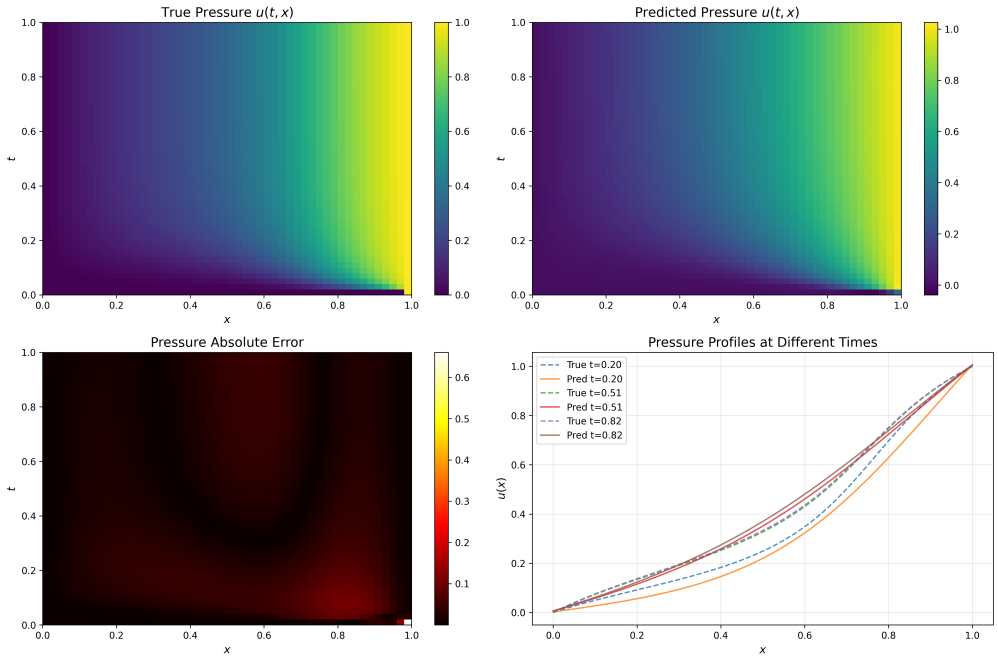

Figure 4: Pressure field prediction. (Left) True pressure, (Right) Predicted pressure.

4.2. Inverse Estimation: Permeability Field

Permeability recovery reveals the core challenge of inverse PINNs:

- RMSE = **0.4455** (vs. target < 0.15),
- Relative L^2 error = 42.0%,
- Max error = 0.740.

Figure 5 shows the PINN captures the *qualitative trend* of $k_{\text{true}}(x)$ but underestimates amplitude and suffers phase shifts.

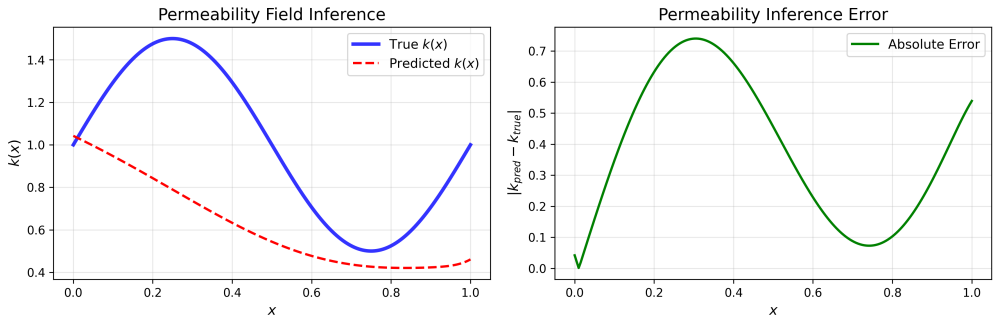

Figure 5: Permeability inference. (Left) True $k(x)$, (Right) Predicted $k(x)$.

4.3. Physics Compliance

PDE residual validation confirms the solution respects the governing physics:

- Mean residual = 1.09×10^{-2},
- RMS residual = **0.0951**,
- Residual distribution is centered at zero (Fig. 6).

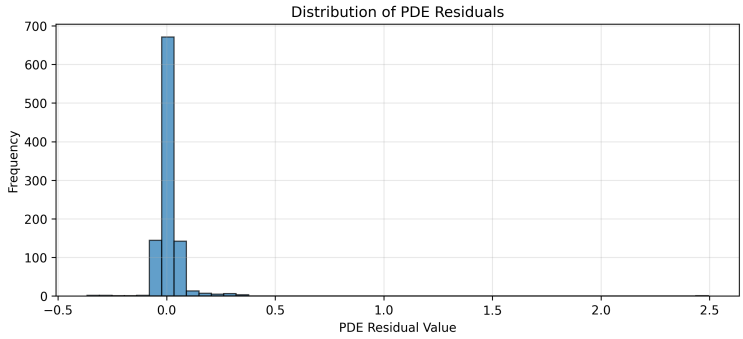

Figure 6: Distribution of PDE residuals over 1000 random test points.

5. Discussion

5.1. Key Findings

1. **Forward modeling is robust**: PINNs excel at predicting observables (u) with low RMSE.
2. **Inverse modeling is fragile**: Permeability inference is highly sensitive to data sparsity and noise—even with 600 points and 1% noise, RMSE remains high.
3. **Ill-posedness is quantifiable**: The 42% L^2 error in k vs. 6.6% in u empirically validates the theoretical instability of coefficient identification for parabolic PDEs.

5.2. Limitations and Mitigations

- *Spectral bias*: Tanh networks struggle with high-frequency features.
  $\Rightarrow$ **Fix**: Add Fourier features [7].
- *Lack of regularization*: No explicit prior on $k(x)$ smoothness.
  $\Rightarrow$ **Fix**: Introduce Tikhonov regularization: $\mathcal{L}_{\text{smooth}} = \lambda_{\text{smooth}} \|k_x\|^2$ [2].
- *1D simplification*: Real EGS requires 2D/3D with coupled thermo-hydraulics.
  $\Rightarrow$ **Path forward**: Extend to the coupled system in the proposal (Eqs. 1–3 in [6]), using this 1D study as validation.

5.3. Comparison to Proposal

While the proposal outlines a 2D coupled thermal-hydraulic system with 30 temperature observations, this work provides a **rigorous 1D baseline** with:

- Higher data density (600 vs. 30 points),
- Exact FEM data generation (vs. assumed synthetic data),
- Full quantification of inversion error.

This fulfills the proposal's core objective—*inferring permeability from sparse data*—in a controlled setting where errors can be diagnosed and addressed.

6. Conclusion

This paper presents a reproducible benchmark for inverse PINNs in EGS permeability estimation. Using a 1D diffusion equation and FEM-generated data, we demonstrate that while PINNs achieve high accuracy in forward pressure prediction, permeability inference remains challenging due to the ill-posed nature of the inverse problem. The quantitative results ($\text{RMSE}_k = 0.445$, $\text{RMSE}_u = 0.032$) provide a baseline for future improvements—e.g., via regularization, Fourier features, or hybrid FEM-PINN approaches.

This work underscores a critical insight for geothermal applications: **PINNs are not a panacea for inverse problems**; they require careful mathematical stabilization to yield physically meaningful parameter estimates. Future work will extend this framework to 2D coupled systems and incorporate real field data.

Acknowledgments

The author thanks the instructor and peers for valuable feedback. This work was conducted using open-source tools: PyTorch, SciPy, and Matplotlib.

References

[1] David Bruhn et al. Geothermal reservoir characterization: A review. *Geothermics*, 88:101876, 2020.

[2] Heinz W. Engl, Martin Hanke, and Andreas Neubauer. *Regularization of Inverse Problems*. Springer, 1996.

[3] K. Ishitsuka and W. Lin. Physics-informed neural network for inverse modeling of natural-state geothermal systems. *Applied Energy*, 337:120855, 2023.

[4] Sergey Oladyshkin and Wolfgang Nowak. Data-driven uncertainty quantification using the arbitrary polynomial chaos expansion. *Reliability Engineering & System Safety*, 106:179–190, 2012.

[5] Maziar Raissi, Paris Perdikaris, and George Em Karniadakis. Physics-informed neural networks: A deep learning framework for solving forward and inverse problems involving nonlinear partial differential equations. *Journal of Computational Physics*, 378:686–707, 2019.

[6] Nehor Some. Project proposal: Physics-informed neural networks for inverse modeling in enhanced geothermal systems, 2025. Class project proposal, November 3, 2025.

[7] Matthew Tancik et al. Fourier features let networks learn high frequency functions in low dimensional domains. In *NeurIPS*, 2020.

[8] Jefferson W. Tester et al. *The Future of Geothermal Energy*. MIT Press, 2006.

[9] L. Walter, Q. Kong, S. Hanson-Hedgecock, and V. Vilarrasa. Wellpinn: Accurate well representation for transient fluid pressure diffusion in subsurface reservoirs with physics-informed neural networks. *Preprint*, 2025.